Resonant Auger Decay of Molecules in Intense X-Ray Laser Fields: Light-Induced Strong Nonadiabatic Effects

Lorenz S. Cederbaum,[1] Ying-Chih Chiang,[1] Philipp V. Demekhin,[1] and Nimrod Moiseyev[2]
[1]*Theoretische Chemie, Universität Heidelberg, Im Neuenheimer Feld 229, 69120 Heidelberg, Germany*
[2]*Schulich Faculty of Chemistry and Minerva Center, Technion—Israel Institute of Technology, Haifa 32000, Israel*
(Received 21 September 2010; published 21 March 2011)

The resonant Auger process is studied in intense x-ray laser fields. It is shown that the dressing of the initial and decaying states by the field leads to coupled complex potential surfaces which, even for *diatomic* molecules, possess intersections at which the nonadiabatic couplings are singular. HCl is studied as an explicit showcase example. The exact results differ qualitatively from those without rotations. A wealth of nonadiabatic phenomena is expected in decay processes in intense x-ray fields.

DOI: 10.1103/PhysRevLett.106.123001 PACS numbers: 33.20.Xx, 31.50.Gh, 41.60.Cr, 82.50.Kx

As far as we know, all excited states of electronic matter like atoms, molecules, and clusters decay, and it is hence not surprising that decay processes have been widely and intensely studied. The advent of x-ray free-electron lasers [1–3] immediately raises the fundamental question of how decay processes behave in intense x-ray radiation. Of particular interest are decay processes of highly excited electronic states which can be excited by a single x-ray photon, where we can directly compare the influence of an intense field with that of the well studied case of a weak field. The resonant Auger (RA) process [4] in which a core electron is excited by a single photon and the resulting highly excited state decays by the emission of an electron has been broadly investigated (see, e.g., [5]) and provides an excellent candidate for this study. The spectrum of the emitted electrons (RA spectrum) depends on the photon energy and on the photon bandwidth, and, importantly, the lifetime of the core-excited state is comparable with pulse durations provided by the x-ray free-electron lasers which allows one to study the competition of time scales [6,7].

Recently, the RA effect has been studied for atoms at high x-ray intensity [7–9], and interesting phenomena have been found like the appearance of multipeak Auger spectra [7]. Multipeak spectra of autoionizing atoms have been predicted to appear for short intense laser pulses [10]. In the present work, we concentrate on molecules and show that an atomiclike picture is inapplicable. Not only the vibrational motion plays a role in the decay as is the case in weak fields, but also the rotational motion becomes uttermost important in intense fields. In particular, even for diatomic molecules, light-induced strong nonadiabatic effects dominate the dynamics of the RA decay which becomes a multidimensional problem in intense x-ray fields. The currently operating x-ray free-electron lasers do not produce so far a monochromatic radiation, and their x-ray pulses consist of many spikes with randomly fluctuating properties [2]. The impact of these problems on the RA effect of atoms has been studied in Ref. [7]. In addition, the x-ray pulse is reshaped during the propagation through a resonant medium [8,9]. In the present work, we concentrate on the physics a single molecule undergoes when exposed to a coherent and monochromatic x-ray pulse. This physics is prerequisite to simulate experiments.

Let us consider a molecule initially in its electronic state Φ_i, which is excited by a laser pulse to a discrete electronic state Φ_d, which is coupled to the continuum and decays by emitting an electron, the Auger electron, of energy E to several final ionic states Φ_f. Following [6], the total wave function of the system as a function of time reads

$$\Psi(t) = \Phi_i \psi_i(t) + \Phi_d \psi_d(t) + \sum_f \int dE \Phi_f \psi_f(E, t), \quad (1)$$

where the respective nuclear wave functions ψ in the various electronic states depend on the nuclear coordinates and on time t and that of the final states also on E. For brevity, we do not show the explicit dependence on coordinates. Inserting $\Psi(t)$ into the time-dependent Schrödinger equation for the total Hamiltonian of the molecule plus its interaction with the laser field and employing as usual the rotating wave and local approximations leads to the matrix equation for the nuclear motion in the dressed electronic states:

$$i\dot{\psi}_{id}(t) = \hat{H}_{id}(t)\psi_{id}(t), \quad (2)$$

where the nuclear wave function $\psi_{id}(t)$ is a column vector with components $\psi_i(t)$ and $\psi_d(t)$. To be specific, we assume a linearly polarized pulse $g(t)\exp(-i\omega_0 t)$ and a diatomic molecule, redefine ψ_d and ψ_f by multiplying them with the phase factor $\exp(i\omega_0 t)$, and obtain [6]

$$\hat{H}_{id} = \hat{T}_N + \begin{pmatrix} V_i & g(t)d\cos\theta \\ g^*(t)d\cos\theta & V_d - i\Gamma/2 - \omega_0 \end{pmatrix}. \quad (3)$$

Here, $\hat{T}_N$ is the common nuclear kinetic energy operator for the stretching motion along the internuclear distance R as well as the rotational motion. V_i and V_d are the potential energy curves of the initial and core-excited decaying

 © 2011 American Physical Society

electronic states, respectively, and Γ is the total resonant Auger decay width. d is the usual dipole transition matrix element, and θ is the angle between the polarization of the pulse and the direction of the transition dipole and thus one of the angles of rotation of the molecule.

Inserting $\Psi(t)$ into the time-dependent Schrödinger equation also determines the final states

$$i\dot{\psi}_f(E,t) = \left(\frac{\Gamma_f}{2\pi}\right)^{1/2} \psi_d(t) + (\hat{T}_N + V_f(R) + E - \omega_0)\psi_f(E,t), \quad (4)$$

where Γ_f is the partial decay width into the fth final electronic state with potential energy curve V_f. The Auger spectrum follows immediately as the sum of the partial spectra, which themselves are determined as the norms of the respective final states after a long time [6]:

$$\sigma_f(E) = \lim_{t\to\infty} \langle \psi_f(E,t) | \psi_f(E,t) \rangle. \quad (5)$$

The dressing of states by the field is qualitatively different from the case of atoms because of the appearance of the two dynamical variables R and θ in the Hamiltonian (3). Without the decay width Γ, the dressed electronic states do not decay, and their energies exhibit a conical intersection at $\theta = \pi/2$ [11]. The impact of such light-induced conical intersections on the dynamics of the system has been recently demonstrated [11]. Because of the presence of Γ in (3), the situation becomes even more intricate. The resulting two potential energy surfaces in R and θ space [obtained by diagonalizing the electronic Hamiltonian $\hat{H}_{id} - \hat{T}_N$ in (3)] are now complex and generally exhibit two intersecting points where the real as well as the imaginary parts of the two electronic energies become degenerate [12]. These analogues of a conical intersection in the continuum have been termed [12] doubly intersecting complex electronic surfaces (DICES). Importantly, the nonadiabatic couplings, i.e., matrix elements of the nuclear momenta along R and θ, between the two dressed electronic states are singular at these intersections [12]. This gives rise to dramatic dynamic effects.

Recently [8,9], it was demonstrated that the role of direct photoionization of the participating states may not be negligible at large pulse intensities. One can incorporate the direct ionization in the theory by adding to the diagonal matrix elements of the Hamiltonian (3) imaginary terms proportional to the respective ionization probabilities [8]. This modification does not change the fact that we have DICES. It may only shift the position of the intersections, but their impact on nonadiabatic effects and the induced coupling between the electronic, rotational, and vibrational degrees of freedom persists. The final ionic state selected for the present calculations is a spectator state where the excited electron does not participate in the decay. In the one-electron approximation, its production by direct photoionization is forbidden. On the other hand, its partial Auger rate is large since only occupied orbitals are involved in the Auger decay. Thus, the Auger channel dominates over the respective direct ionization, which is excluded from the calculations of the Auger spectrum. In order to keep our presentation transparent, we neglect direct photoionization in the following. We would like to demonstrate the dynamic effects of DICES for a realistic example, the HCl molecule. We have chosen HCl because of several reasons. First, all the input data needed for the involved calculations of the dynamics are known in the literature [13,14]. Second, the weak-field RA of HCl has been measured [14]. Third, and importantly, both V_d and the V_f chosen are dissociative, implying that the spectrum will be rather simple and not be complicated by the appearance of many quasidiscrete peaks which are difficult to analyze.

The potential curves of HCl are shown at the top of Fig. 1. The dressed potential surfaces shown in Fig. 1 have been calculated by using (3) for the plateau of a square pulse $g(t)$ of intensity 2.2×10^{17} W/cm^2 and a frequency which brings the potential curves V_d and V_i into resonance at the minimum geometry of the latter ($\omega_0 = 200.8$ eV). The real parts of the surfaces show a seam of degeneracy along a range of θ which depends on Γ: The larger Γ, the longer the seam. The imaginary parts of the surfaces have a complementary seam of degeneracy at a value of $\Gamma/2$, such that the complex surfaces intersect at exactly two points which are at the edges of the seams. We note that the imaginary surfaces which reflect the decay of the dressed states now are strongly dependent on R and θ in contrast to the constant value of Γ (76.5 meV [13]) of the original decaying state V_d.

We have performed several computations on the full dynamics of (3) and (4) for HCl by using square and Gaussian pulses. To be able to carry out the two-dimensional calculations on the coupled complex surfaces, we had to employ an efficient method and code [15,16]. Since Gaussian pulses are often used in the literature, we will concentrate on them. Figure 2 shows the total Auger yield as a function of the peak intensity for a longer (FWHM of 6.6 fs) and a shorter (FWHM of 3.3 fs) pulse. The inset depicts the results of an atomic model of HCl where R is kept fixed at the minimum of V_i ($R = 1.28$ Å) and $\theta = 0$. The atomic case is well understood [7]: If the pulse is sufficiently short in comparison with the Auger lifetime ($\tau = 1/\Gamma = 8.6$ fs), then when the pulse is over the atom has a finite probability of being in its ground state, and the minima and maxima in the total yield are related to the number of half Rabi cycles the atom manages to complete during the x-ray pulse. Next we compare with calculations of the dynamics where R is a dynamic variable, but θ is kept fixed at 0. We call the approach "no DICES." The results in Fig. 2 already show substantial deviations from the atomic model. The extrema of the oscillations still crudely approximate those of the atomic

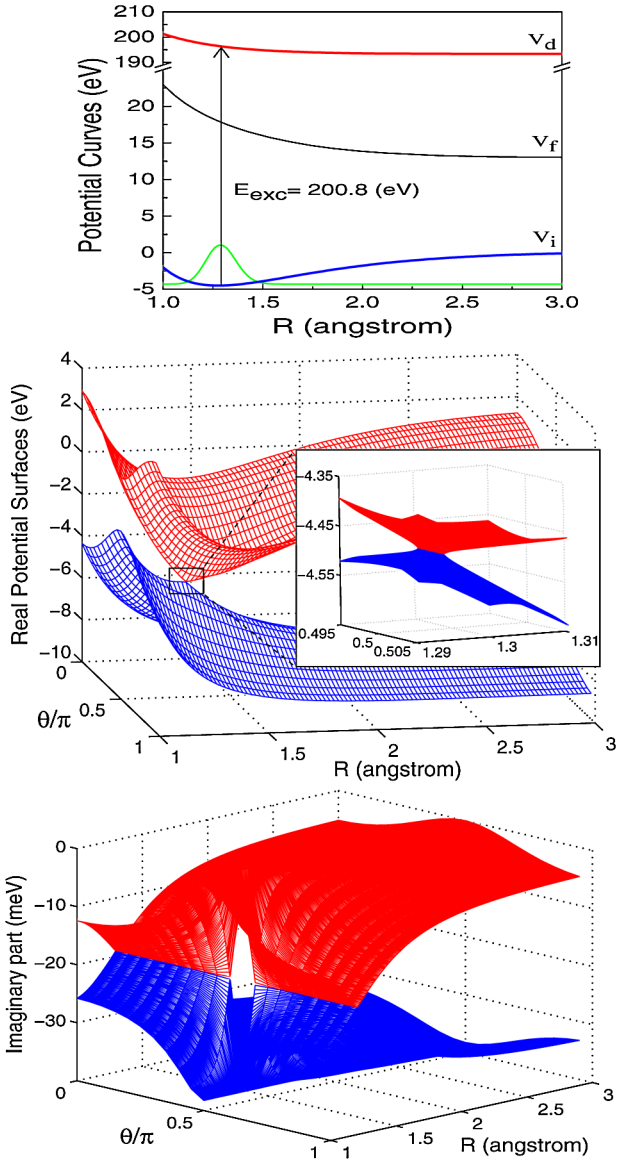

FIG. 1 (color online). Potential curves and surfaces. Upper panel: Potential energy curves of the ground state (V_i) and the decaying Cl $2p \rightarrow \sigma^*$ core-excited state of HCl (V_d) and the final $2\pi^{-2}\sigma^*$ state of HCl^+ used in this work (taken from Refs. [13,14]). Other panels: When dressed by an x-ray laser light of frequency $\omega_0 = 200.8$ eV and intensity 2.2×10^{17} W/cm^2, the ground and decaying potentials become doubly intersecting surfaces in R and θ space. Their real part is shown in the middle and the imaginary part in the lower panel.

model, but their amplitudes are much smaller and the yield is always well below 1. Obviously, a two-level model, appropriate for atoms, is not applicable here. The deviation from the atomic model is even more dramatic if we compare with the results of the full dynamics (marked in Fig. 2 as "DICES"). Now, the oscillations have disappeared and we find a monotonically increasing yield with intensity. This behavior is due to the strong nonadiabatic effects

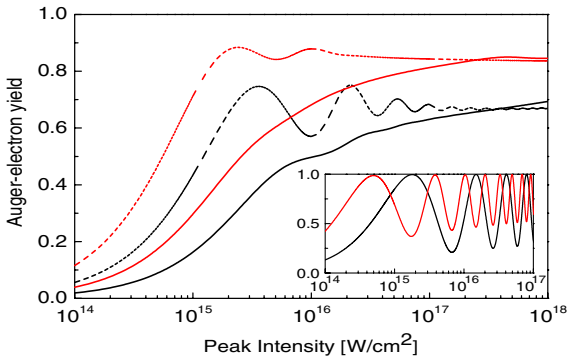

FIG. 2 (color online). The total RA yield as a function of peak intensity for 3.3 and 6.6 fs Gaussian pulses. The solid lines show the exact results (DICES) and the broken lines the no DICES results. The inset shows the results for an atomic model of HCl. (6.6 fs in red; 3.3 fs in black.)

produced by the DICES. The situation is extremely far from an effective two-level model.

The computed Auger spectra are collected in Fig. 3 for the 3.3 fs pulse. In the upper left panel, the weak-field result is depicted for which the upper panel of Fig. 1 applies. The vibrational wave function of V_i is excited vertically to the dissociative potential curve V_d and starts to decay while it propagates towards dissociation into a H atom and a core-excited Cl atom which decays into Cl^+ and an Auger electron. Consequently, one sees a narrow atomic peak and a molecular peak which stems from the early decay when core-excited HCl is still a molecule. This situation has been studied both experimentally and theoretically [14]. For weak fields the structure of the spectrum is independent of whether we have used DICES or not. The situation changes clearly if the field intensity is increased. For 2.2×10^{17} W/cm^2 (upper right panel) the no DICES spectrum exhibits peaks reminiscent of the atomic model of HCl, while the exact (DICES) spectrum shows interesting wings but no peaks. The situation is qualitatively similar at 10^{18} W/cm^2 except that the peaks in the no DICES spectrum have moved apart and the wings of the exact spectrum have spread by several eV. The last panel shows the spectrum at 1 eV above resonance ($\omega_0 = 201.8$ eV). The asymmetry of the spectrum has strongly changed as the surfaces intersect at larger values of R, changing the topology of the DICES and thus the impact of the nonadiabatic effects.

Before the pulse arrived, the molecules were in their ground state, i.e., isotropically oriented. How does this situation change for the remaining molecules which did not decay after the pulse has left? The upper panel of Fig. 4 shows that the distribution remains isotropic at weak pulse intensities of 10^{14} W/cm^2 (see the inset) and that this changes dramatically at larger intensities when the DICES become effective. Obviously, there is a very large number of angular momenta quanta exchanged during the dynamics in order to allow for the resulting distribution to

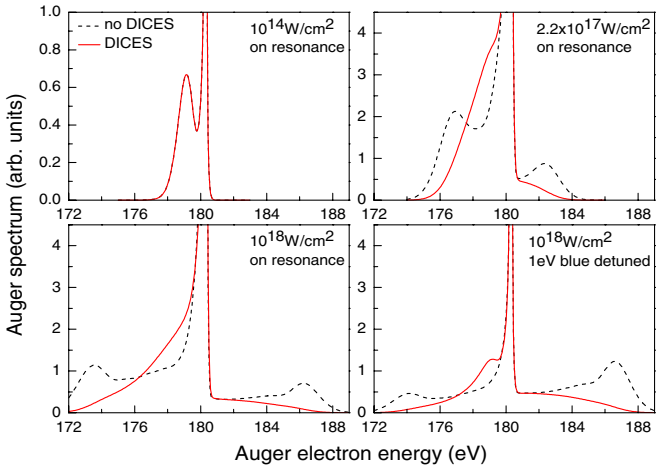

FIG. 3 (color online). Resonant Auger spectra for a 3.3 fs Gaussian pulse. Solid red lines are exact results (DICES); broken black lines are no DICES results (in each panel the scale refers to the exact results and the maxima of the spectra are set equal). Upper left panel: Weak field (10^{14} W/cm^2). The red and black curves are indistinguishable. Upper right panel: Stronger field (2.2×10^{17} W/cm^2). Lower left panel: Strong field (10^{18} W/cm^2). Lower right panel: As in the former panel, but with +1 eV off resonance detuning ($\omega_0 = 201.8$ eV).

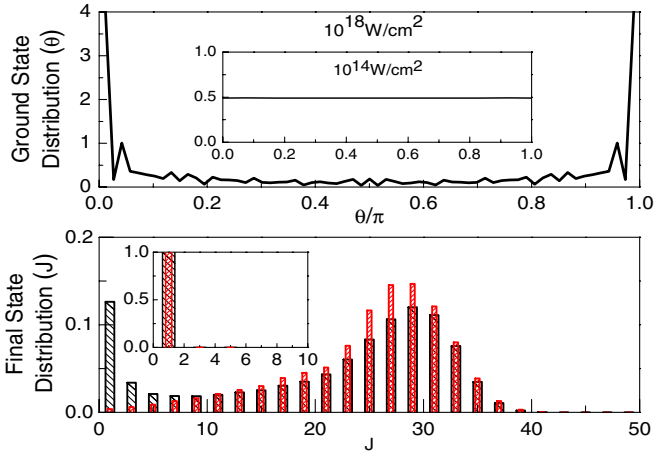

FIG. 4 (color online). Impact of the DICES on rotations. Upper panel: Distribution of the remaining molecules which did not decay as a function of θ (at 140 fs after the pulse maximum). Before the pulse (3.3 fs pulse with 10^{18} W/cm^2), the distribution was isotropic. The weak-field result (10^{14} W/cm^2) is shown in the inset. Lower panel: The distributions of angular momenta J of the decay products H and Cl^+ for different energies of the Auger electron, in red for the atomic peak (180.3 eV) and in black for the molecular peak (179 eV); see Fig. 3. The inset shows the weak-field results.

occur where a fraction of the molecules are sharply aligned and the rest are organized in small groups around some values of θ. The large impact of the nonadiabatic dynamics which leads to the excitation of angular momenta is best documented in the distribution of the total angular momenta J of the H atom and the Cl^+ produced by the RA process of HCl. This distribution is shown in the lower panel of Fig. 4 for two energies of the Auger electron, selected to be on the atomic peak (180.3 eV) and on the molecular peak (179 eV) in the Auger spectra of Fig. 3. For weak fields the distribution is essentially at $J = 1$ as expected from single photon absorption selection rules (see the inset). At stronger fields the distribution is different whether one collects the products corresponding to the atomic or the molecular peak. In both cases it is astonishing that the distribution peaks around rather large values of J and that J values up to above 50 contribute. We remind the reader that the no DICES approach does not give rise to rotational coupling at all.

In conclusion, the nonadiabatic couplings induced by intense x-rays between the initial electronic state and the state decaying by RA are singular even for diatomic molecules, and this leads to strong nonadiabatic effects and to substantial interactions of fragmentation (vibrations if the decaying state is nondissociative) and rotations. In polyatomics the off-diagonal element in (3) will contain $d_\parallel \cos\theta + d_\perp \sin\theta$, and, owing to the different dependence of $d_\parallel$ and $d_\perp$ on the various nuclear coordinates, other nuclear degrees of freedom than rotations may play a substantial role. Because of the immense induced coupling between the states, other states which are not in resonance become less important, but if needed, the present theory can easily be extended to include more states. In general, one can expect a wealth of nonadiabatic effects which can be controlled by varying the frequency, the pulse duration, and the pulse intensity. RA decay induced by a pump pulse has the advantage that the decay itself carries via its products the essential information and thus replaces a probe pulse often needed otherwise.

This research was supported in part by the IMPRS at the MPIK, Heidelberg.

[1] K. Tiedtke *et al.*, New J. Phys. **11**, 023029 (2009).
[2] P. Emma *et al.*, Nat. Photon. **4**, 641 (2010).
[3] T. Tanaka and T. Shintake, http://www-xfel.spring8.or.jp/.
[4] G. S. Brown *et al.*, Phys. Rev. Lett. **45**, 1937 (1980).
[5] G. B. Armen *et al.*, J. Phys. B **33**, R49 (2000).
[6] E. Pahl *et al.*, Z. Phys. D **38**, 215 (1996).
[7] N. Rohringer and R. Santra, Phys. Rev. A **77**, 053404 (2008).
[8] J.-C. Liu *et al.*, Phys. Rev. A **81**, 043412 (2010).
[9] Y.-P. Sun *et al.*, Phys. Rev. A **81**, 013812 (2010).
[10] K. Rzaznewski *et al.*, Phys. Rev. A **31**, 2995 (1985).
[11] M. Sindelka *et al.*, J. Phys. B **44**, 045603 (2011).
[12] S. Feuerbacher *et al.*, J. Chem. Phys. **120**, 3201 (2004).
[13] A. D. Pradhan *et al.*, J. Chem. Phys. **95**, 9009 (1991); D. Shaw *et al.*, J. Phys. B **17**, 1173 (1984).
[14] H. Aksela *et al.*, Phys. Rev. A **41**, 6000 (1990); A. Menzel *et al.*, Chem. Phys. Lett. **258**, 265 (1996).
[15] H.-D. Meyer *et al.*, Chem. Phys. Lett. **165**, 73 (1990).
[16] G. A. Worth, M. H. Beck, A. Jäckle, and H.-D. Meyer, The MCTDH package; see http://mctdh.uni-hd.de.